A New Approach for Improving the Load Current Characteristic of Cascaded Magnetic Flux Compression Generator

Mohammad Jafarifar, Behrooz Rezaeealam*, and Ali Mir

Department of Electrical Engineering
Lorestan University, Khorramabad, Iran
*rezaee.bh@lu.ac.ir

Abstract – Helical magnetic flux compression generators (HFCGs) are widely used to generate extremely high-power pulses. Two most important output characteristics of HFCGs in their use as pulsed power generators are maximum value of load current and the rise time of that current. In this paper, an approach is proposed to improve the output characteristic of a Cascaded-HFCG. The approach is based on time-varying primary winding of dynamic transformer and addition of a gradually incremental resistance in series with the first stage winding. It is demonstrated analytically using simulation results that the output current and its rise-time improve by minimizing energy returned from secondary winding to primary winding of dynamic transformer. The results are compared to conventional Cascaded-HFCG that has a non-destructive winding in its structure. A finite element model is considered to calculate the self-inductances, mutual inductance and resistances of the generator. A new approach is proposed to gradually increase in the resistance of primary winding of dynamic transformer.

Index Terms ─ Dynamic transformer, explosive charge, helical magnetic flux compression generator, incremental resistance, load characteristic.

I. INTRODUCTION

Helical magnetic flux compression generators (HFCG) are widely used to produce very high current pulses in the recent past decades. These generators convert the chemical energy of explosive charge into magnetic energy in the form of current pulses. They are used in a variety of applications like nuclear research, X-Ray source, high power microwave, high power laser, rail gun, and so on. Some applications of HFCGs require shorter pulse width (shorter rise-time), higher voltage, higher current, higher energy gain and higher instantaneous power delivered to load [1]. Several approaches are proposed in literatures to achieve these requirements. For example, an increase in the axial length of winding increases current gain and energy gain of the generator but causes wider pulse width [2].

Another approach to get the higher current and energy gain is to increase the diameter of armature, which cause increase in cost and explosive pressure [2]. As mentioned, many applications require a rise-time of output current pulses in the range of one microsecond or less. In order to achieve shorter pulse width (less rise-time of pulse), the inductance of winding should be rapidly reduced (dL/dt reaches a maximum value). In the past few decades, several approaches have been proposed to increase the rate of inductance changing in HFCGs. One approach that is especially useful in larger HFCGs is to use areal or simultaneous initiation of the explosive charge [3], which may be achieved in either outside-in or inside-out detonations. Generally, the outside-in initiation is used for high magnetic field experiments [4]. The inside-out simultaneous initiation systems are successfully used in several generator designs [4]. Another approach is to taper the stator diameter to an angle less than the armature expansion angle. This technique is used in larger generators as well. Disadvantages of this approach include finite length systems and the difficulties in fabrication and assembly of the tapered stator [4]. Short pulse width can usually be achieved by using a conventional HFCG coupled with a pulse-forming circuit, such as an opening switch or fuse. Opening switches are difficult to design and fabricate and add greatly to the complexity of the experiment [5]. In [6], a new method is proposed to reach an arbitrary pulse width using two explosive current-opening switches (EOS) combined with HFCG. An EOS is used to form the leading edge of current pulse, while an explosive current interrupter (EOI) switched in-series to electrical circuit provides the duration of current pulse and the formation of its trailing edge. The most important advantage of this method is the production of a pulse with controlled amplitude and duration with a trapezoidal shape. Because of existence of two EOSs in this method, its manufacturing is very complicated, time consuming and expensive.

The first idea to overcome the aforementioned problems was to use inductively coupled Cascaded generators using air-cored transformer [7]. After that, in

1979, among several ideas and opinions, Chernyshev proposed the use of a dynamic transformer and its combination with Cascaded generator [8]. A Cascaded generator consists of two or more FCGs connected in-series with an air transformer or dynamic transformer, where each FCG is the load of the previous generator. A schematic of Cascaded-HFCG is shown in Fig. 1. It is composed of two conventional HFCGs, which are coupled magnetically using dynamic transformer.
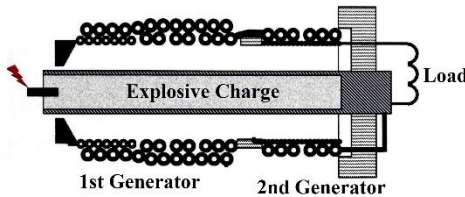

Fig. 1. Schematic of Cascaded Helical Magnetic Flux Compression.

The electrical equivalent circuit of Cascaded-HFCG after starting the explosion is shown in Fig. 2.
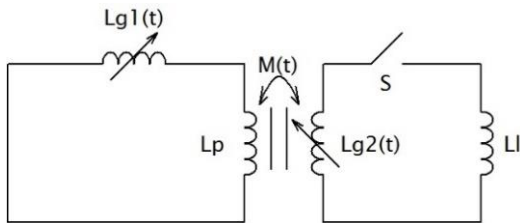

Fig. 2. Electrical Circuit of Cascaded-HFCG.

In the circuit shown above, $L_{g1}(t)$ is winding of first stage, L_P is primary winding of dynamic transformer, $L_{g2}(t)$ is winding of second stage (secondary of dynamic transformer) and L_l is load inductance. A seeding system (usually a capacitor bank) introduces an initial magnetic flux into generator by injecting current directly into first stage winding. When the explosion starts, the armature is expanded, and the injected flux is compressed. At the end of the first stage operation, switch S is closed, and the magnetic flux is trapped by $L_{g2}(t)$ using a dynamic transformer. At the same time, load current appears and increases rapidly to form a current pulse. The rise-time of load current is smaller than that of first stage current due to lower axial length of $L_{g2}(t)$ compared to $L_{g1}(t)$. Another advantage of Cascaded-HFCG is that it can be used as a voltage pulse generator with arbitrary amplitude because of the existence of step-up transformer (dynamic transformer) in its structure [8].

Actually, a Cascaded-HFCG is composed of two conventional HFCGs, which are connected in series and coupled magnetically; thus, its efficiency is expected to be a number close to the product of efficiency of each individual HFCG. However, experimental results show that the efficiency of Cascaded-HFCG is about 30% less than the expected value [2]. One of the reasons of this lower efficiency is magnetic flux loss at the moment of flux trapping in second stage (this moment is called crowbar). Adequately, high mutual inductance between dynamic transformer windings can decrease flux losses and consequently increase the generator efficiency. There are many factors that maximize mutual inductance between two windings, such as turns number of windings, pitch of winding, axial length of windings and so on [9]. Although, high mutual inductance decreases magnetic flux losses, it can increase transferred energy between two windings. As we know, in Cascaded-HFCGs, after starting the second stage operation, the first stage current is still ongoing. Given that two stages are magnetically coupled through dynamic transformer, a part of energy returns to the first stage. Since there is no electrical connection between load and first stage winding, the returned energy leads to increase in current of first stage winding instead of reaching to load. In [10], a flux-trapping HFCG is considered, which is structurally similar to Cascaded-HFCGs. Simulation results show that close to the end of the generator operation, mutual inductance between main winding (which is similar to second stage winding in Cascaded-HFCG) and field winding (which is similar to first stage winding in Cascaded-HFCG) is high enough for a great amount of energy to return to the field winding circuit. The returned energy causes an increase the current of field winding more than the usual (as can be seen from Fig. 5 of [10]). It should be noted that in the described flux-trapping HFCG, the field winding only covers the first 50% of the main winding, which helps to decrease the coupling between the two windings before an appreciable amount of energy is transferred to the field-winding circuit. In [11], a Cascaded-HFCG is considered, in which primary winding of dynamic transformer covers 100% of the second stage winding. Simulation results show that due to the high amount of energy returned to the first stage winding, its current increases irrationally (Fig. 6 in [11]).

It can be concluded from the above discussion that one of the main issues about the lower efficiency of Cascaded-HFCG is the increase in first stage current more than the common value after crowbar instance and increase in ohmic losses. In [12], it is proposed to rapidly cut off current of the first stage by an EOS. On the other hand, it is shown that in this case, a surge voltage is produced in the generator, which causes electrical break down in generator insulators [13].

This paper proposes an approach to overcome the problems described above. In order to minimize the energy returned to the first stage, mutual inductance between two windings of dynamic transformer should tend to a very small value after starting the second stage operation. In conventional Cascaded-HFCG, the two

windings of dynamic transformer do not essentially decouple during the generator run time. If each turns of primary winding of dynamic transformer wipes out simultaneously with turns of second stage winding and armature expansion, the two windings can decouple more quickly, and the returned energy decreases significantly. Actually, the primary winding of the dynamic transformer should have time-varying behavior like the other windings of generator ($L_P \rightarrow 0$). In the case of time-varying L_P, the self-inductance of first stage winding reaches zero at the end of generator operation (in the conventional Cascaded-HFCG, the self-inductance of L_P is a non-zero value), therefore, the maximum value of the current of first stage winding increases too. To prevent the unusual increasing in the first stage current, a gradually incremental resistance should be introduced in-series with L_P. Added resistance restricts the maximum value of first stage current, which causes an increase in the load current. These claims are proved analytically and using simulation results. The mathematical model proposed in [11] is used for simulation of Cascaded-HFCG. Resistances of windings are calculated by the method presented in [14]. Time varying self-inductances and mutual inductance are calculated using finite element method (FEM) and validated by comparing with 2-D filamentary method described in [15].

II. MODELING OF CASCADED-HFCG

According to the model proposed in [11], the operation of Cascaded-HFCG can be divided into two distinct phases. The first phase of the operation begins by starting the explosion. Kirchhoff's voltage equation for the loop containing first-stage winding can be written as:

$$[L_{g1}(t)+L_p]\frac{dI_{g1}(t)}{dt}+[R_{g1}(t)+\alpha_1\frac{d(L_{g1}(t)+L_p)}{dt}]I_{g1}(t)=0, \quad (1)$$

where α_1 is the flux conservation coefficient, accounting for intrinsic flux losses in the first stage.

The second phase begins after the closure of switch S and lasts until the end of generator operation. Kirchhoff's voltage equation for the loops are as follows:

$$[L_{g1}(t)+L_p]\frac{dI_{g1}(t)}{dt}+[R_{g1}(t)+\alpha_1\frac{d(L_{g1}(t)+L_p)}{dt}]I_{g1}(t)+M(t)\frac{dI_{g2}(t)}{dt}+I_{g2}(t)\frac{dM(t)}{dt}=0, \quad (2)$$

$$[L_{g2}(t)+L_1]\frac{dI_{g2}(t)}{dt}+[R_{g2}(t)+R_1+\alpha_2\frac{dL_{g2}(t)}{dt}]I_{g2}(t)+M(t)\frac{dI_{g1}(t)}{dt}+I_{g1}(t)\frac{dM(t)}{dt}=0. \quad (3)$$

In (3), α_2 is the flux conservation coefficient accounting for intrinsic flux losses of the second stage. By solving the equations above, the time-varying current in the circuits can be calculated. However, the time variations of the inductances and resistances of windings should be obtained and the values of α_1 and α_2 should be determined in advance.

III. INDUCTANCE AND RESISTANCE CALCULATION

While there are many analytical formulas for the calculation of self-inductance and mutual inductance of the two air-cored helical windings, there is almost no explicit formula that produces accurate results when a magnetic core such as an aluminum armature is added inside the windings. The reason for this is that inductance calculation in the presence of magnetic core requires the use of formulas involving elliptic integrals or infinite series, which can be very complicated. Numerical methods can be used to avoid the calculation these complicated and time-consuming integrals.

In [14], a zero-dimensional method of calculating time varying inductances based on working volume collapse during armature expansion is introduced. This method is very simple and fast and is thus sufficient for designing purpose.

In [15], a method called 2-dimensional filamentary is introduced for the calculation of the self-inductance and mutual inductance of HFCG. According to this model, the armature and both windings of the generator are decomposed into the same number rings. The inductance of each winding involves the superposition of the self-inductance of rings and mutual inductance between them. In this model, the higher number of rings for armature provide further accuracy in inductance calculation, but this is more time-consuming, and the simulation becomes more complicated.

In [16], a 2-dimentional method based on the concept of equivalent impedance is proposed. Equivalent impedance can be calculated in each step of the generator operation through the division of voltage phasor by current phasor in an equivalent frequency. This method is only proposed for the calculation of self-inductance of conventional HFCG.

The most useful formula for the computation of self-inductance of a system involves calculating the total magnetic energy using (4):

$$E_m=\int_V \frac{B^2}{2\mu_0}dv=\frac{1}{2}\int_V \bar{A}.\bar{J}dv,$$

$$E_m=\frac{1}{2}LI^2. \quad (4)$$

For a linear magnetic system, the volume integral of (4) can be calculated analytically, but for nonlinear systems, there is no analytical solution for this integral and it should be calculated using numerical methods [10].

An appropriate method to calculate the mutual inductance of the two windings is to consider the system as a four-terminal device. A known current is applied at the input terminals of device (one of the windings), which induces a voltage across the output terminals (the other winding). The induced voltage can be calculated

from the magnetic potential vector using Faraday's law. The calculated voltage can be used to compute the mutual inductance via:

$$\text{mutual inductance} = \frac{\text{induced voltage}}{j(\text{angular frequency of supply}) \times (\text{applied current})}. \quad (5)$$

Considering (4) and (5), in order to achieve self and mutual inductances, it is necessary to calculate magnetic vector potential (A). Using the Maxwell equations, the magnetic potential vector can be written in the form of (6) for a system with certain boundary conditions:

$$\nabla^2 \bar{A} = -\mu_0 \bar{J}, \quad (6)$$

where μ_0 represents the magnetic permittivity of the vacuum, $\bar{J} = \sigma \bar{E} = -\sigma(\partial \bar{A}/\partial t)$ represents the vector of current density and σ special electrical conductivity. By replacing $\bar{J}$, the (6) obtains in the form of (7):

$$\nabla^2 \bar{A} - \sigma \mu_0 \frac{\partial \bar{A}}{\partial t} = 0. \quad (7)$$

In other regions where there is no current ($\sigma = 0$), (6) converts to the Laplace equation:

$$\nabla^2 \bar{A} = 0. \quad (8)$$

A helical flux compression generator is cylindrical and thus, using a cylindrical coordinate system is suitable for its analysis. Considering the symmetry of the helical generators, (6) can be expressed in the various parts of the generator in the form of (7):

$$\frac{\partial^2 A}{\partial z^2} + \frac{\partial^2 A}{\partial r^2} + \frac{1}{r}\frac{\partial A}{\partial r} - \frac{A}{r^2} = 0, \qquad \textit{for free space}$$

$$\frac{\partial^2 A}{\partial z^2} + \frac{\partial^2 A}{\partial r^2} + \frac{1}{r}\frac{\partial A}{\partial r} - \frac{A}{r^2} - \sigma\mu_0\frac{\partial A}{\partial t} = 0, \qquad \textit{for armature} \quad (9)$$

$$\frac{\partial^2 A}{\partial z^2} + \frac{\partial^2 A}{\partial r^2} + \frac{1}{r}\frac{\partial A}{\partial r} - \frac{A}{r^2} - \sigma\mu_0\frac{\partial A}{\partial t} = -\sigma\mu_0 J. \quad \textit{for windings}$$

By solving (9), the magnetic potential vector is calculated and using the (4) and (5) we can obtain the self and the mutual inductance.

In this paper, the self-inductance and mutual inductance of windings are calculated using FEM. The two stages of the generator, dynamic transformer and armature are modeled in 3-D as shown schematically in Fig. 3. The modeled domain is surrounded by a region of infinite elements, which is a way to truncate a domain that stretches to infinity. Each winding is modeled as a hollow cylinder that can be considered as a multi-turn winding. The armature is modeled as an aluminum hollow cylinder that can be considered as a single-turn coil passing the current of generator stages. The free space between windings and armature (called working volume) is considered as air.

Figure 4 shows a typical 2D axisymmetric schematic for the modeled Cascaded-HFCG demonstrated in Fig. 3.

Self-inductance calculation of the first-stage winding can be carried out by neglecting the second-stage winding. A known current (for example 1A) is introduced to the first-stage winding. Using (4), the time-varying inductance profile can be calculated. Figure 5 shows the calculated time-varying self-inductance profile of the first-stage winding using the described FEM. In order to verify the validation of the calculated profiles, a simulation is performed using the 2-D filamentary method described in [15] and the results are compared. As we can see, there is an approximately good agreement between the calculated inductance profile using the FEM method and 2-D filamentary method.
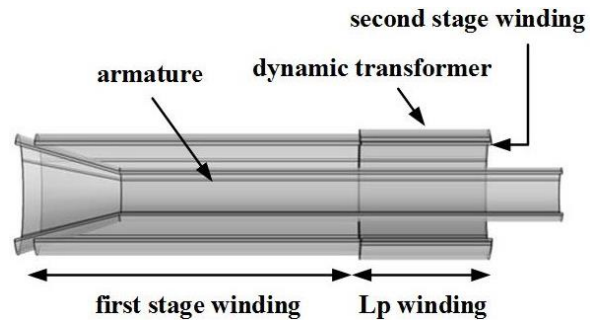

Fig. 3. FEM model of Cascaded-HFCG used to calculate inductances.
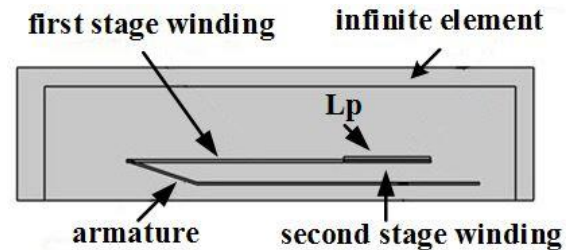

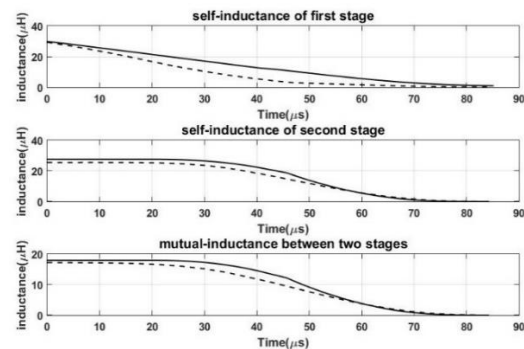Fig. 4. 2D axisymmetric for the modeled Cascaded-HFCG.

Fig. 5. Calculated time-varying inductances: (solid line) for FEM method; (dashed line) for 2-D filamentary method.

Inductance calculation procedure for second-stage winding is similar to the one described for the first stage.

First-stage winding is the neglected and a known current is fed to second-stage winding. The self-inductance profile of second-stage winding is similar to that of the first stage. But the difference is that during first-stage operation, there is no contact between second-stage winding and armature, as a result of which inductance is approximately constant. After closure of switch S, all turns of the winding are wiped out one by one and inductance tends to zero at the end of the generator operation. Figure 5 shows the calculated time-varying self-inductance of second-stage winding.

There are two accurate methods in literature to calculate the mutual inductance of two windings in the presence of armature. The first one is to fabricate the generator and measure inductance. This method is very time-consuming and expensive. Also, it is only possible to measure initial inductance experimentally because there is no device to measure mutual inductance during the generator operation. The second method is numerical simulation, such as electromagnetic field (EF) solver. In our model, the first-stage winding is fed by a current as the input of the four-terminal device. The second-stage winding is considered to be open-circuit and the induced voltage across its terminals is calculated using FEM. Finally, the mutual inductance is calculated using (5). Figure 5 shows time-varying mutual inductance of Cascaded-HFCG calculated by FEM.

In [14], a simple method is proposed to calculate the resistance for each winding of HFCG,

$$R(t)=R_{dc}(t) \times K_T \times K_{skin} \times K_{proximity}. \tag{10}$$

In this equation, $R_{dc}(t)$ is the DC resistance of winding, K_T is the temperature correction of conductivity, K_{skin} is correction for skin effect, and $K_{proximity}$ is correction for proximity effect. In our FEM model, a known current (a simple current source of 1A) is connected in series to each winding and electrical voltage between its two terminals is calculated using FEM. The DC resistance of the windings is equal to the electrical voltage between terminals over the applied current (in this case, 1A). The equation for the calculation of these corrections is described in [14].

IV. ANALYTICAL SOLUTION

In this section, an analytical analysis is performed to describe an approach to increase the load current of Cascaded-HFCG and decrease the rise-time of load current. The results are validated by simulation in the next section. For simplification, ohmic resistances of windings and armature are assumed to be negligible. Suppose that at the starting of generator operation, initial flux $\Phi(0)$ is introduced to first-stage winding by initial energy supply. For time interval $(0, t_1)$, where t_1 is crowbar time of the second stage, flux equation for the left loop of Fig. 2 can be written as:

$$\Phi(0)=(L_p+L_{g1}(0))I_{g1}(0).$$
$$\Phi(t)=(L_p+L_{g1}(t))I_{g1}(t)=\Phi(0). \tag{11}$$

At the end of the flux compression procedure in the first stage, self-inductance of first-stage winding vanishes ($L_{g1}(t_1) \to 0$). Thus, (11) changes as follow:

$$\Phi(t_1)=L_pI_{g1}(t_1)=\Phi(0). \tag{12}$$

After the closure of switch S at the moment t_1, the following system of flux equations is valid for two loops of Fig. 2:

$$L_pI_{g1}(t)+M(t)I_{g2}(t)=L_pI_{g1}(t_1), \tag{13}$$

$$(L_{g2}(t)+L_l)I_{g2}(t)+M(t)I_{g1}(t)=M(t_1)I_{g1}(t_1). \tag{14}$$

The right term in (14) is magnetic flux trapped by second stage due to mutual inductance between the windings. Solving (13) and (14) using (12), we can find the current of second stage of the generator:

$$I_{g2}(t)=\Phi(0)\frac{\frac{1}{L_p}\left[M(t_1)\text{-}M(t)\right]}{L_l+L_{g2}(t)\left(1\text{-}\frac{M^2(t)}{L_pL_{g2}(t)}\right)}. \tag{15}$$

At the end of the generator operation, the value of $L_{g2}(t)$ and $M(t)$ tend to zero, and the (15) changes as follows:

$$I_{g2}(t_{end})=\Phi(0)\frac{\frac{1}{L_p}M(t_1)}{L_l} = \Phi(0)\frac{M(t_1)}{L_pL_l}. \tag{16}$$

It can be concluded from (16) that the final value of load current depends on three factors. The impact of $\Phi(0)$ and $M(t_1)$ on load current is considered in many existing articles [9]. The third effective factor on load current is the inductance of primary winding of dynamic transformer (L_P). It is obvious that smaller L_P results higher load current. According to the design criteria's, and to maximize the flux trapped by dynamic transformer, L_P should not have very small initial value. If inductance of L_P decreases after the crowbar of second stage operation and simultaneously with armature expansion, the load current increases consequently. In a conventional Cascaded-HFCG, inductance of L_P is approximately constant; however, a destructive structure using a very thin explosive substrate located over or under the L_P can sweep out turns of L_P and cause to inductance of L_P to decrease ($L_P \to 0$) [13].

As previously mentioned, the current of the first stage winding after second stage crowbar causes a decrease in the efficiency of Cascaded-HFCG and consequently decreases load current. To overcome this problem, we propose adding a gradually incremental resistance in-series with L_P. The advantage of added resistance is explained analytically in the following. Let (3) be rearranged as:

$$[L_{g2}(t)+L_1]\frac{dI_{g2}(t)}{dt}+[R_{g2}(t)+R_1+\alpha_2\frac{dL_{g2}(t)}{dt}]I_{g2}(t)$$

$$=-M(t)\frac{dI_{g1}(t)}{dt}-I_{g1}(t)\frac{dM(t)}{dt}. \quad (17)$$

In (17), $I_{g1}(t)$ has a positive sign and $dM(t)/dt$ is negative during the generator operation; thus, the term $-I_{g1}(t)(dM(t)/dt)$ (shown as term A for convenience) is a positive quantity for the whole duration of generator operation. In return, $-M(t)(dI_{g1}(t)/dt)$ (term B) can be considered in two cases as follows:

a) In conventional Cascaded-HFCG (with no added series resistance), $I_{g1}(t)$ increases for the whole duration of generator operation, so $dI_{g1}(t)/dt$ has positive sign. On the other hand, $M(t)$ is positive too, so the sign of term B becomes negative. In this condition, the right side of (13) is equal to A-B.

b) Adding series resistance with L_p cause current to become descending and $dI_{g1}(t)/dt$ gets negative sign in this case, so the sign of term B becomes positive and the right side of (17) is equal to A+B.

It is obvious that for the case (b), the right side of (17) has a greater value than the case (a), due to which load current becomes greater.

Another advantage of added incremental resistance is the decreasing in rise-time of load current. Ohmic resistance of load and second stage can be negligible, so (17) can be written as:

$$\frac{dI_{g2}(t)}{dt}=\frac{-M(t)\frac{dI_{g1}(t)}{dt}-I_{g1}(t)\frac{dM(t)}{dt}-I_{g2}(t)\frac{dL_{g2}(t)}{dt}}{L_{g2}(t)+L_1}. \quad (18)$$

With the same analysis as before, if $dI_{g1}(t)/dt$ is a negative quantity, the numerator of (18) becomes larger and this means smaller rise-time of current. This is one of the goals of the optimization of Cascaded-HFCG.

V. SIMULATION RESULTS AND DISSCUSION

As previously mentioned, L_p has a great impact on generator efficiency in Cascaded-HFCGs because of its participation in energy transfer to second stage winding and load. The (16) shows that if each turn of L_p is wiped out simultaneously with armature operation and second stage winding, the load current increases. On the other hand, coupling between L_p and second stage winding decreases gradually; thus, the returned energy to L_p decreases, which can increase the generator efficiency. The self-Inductance profile of first stage winding for the case of time varying L_p which calculated using FEM is shown in Fig. 6.
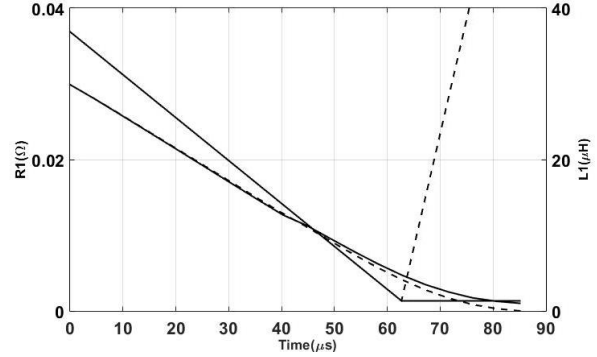

Fig. 6. Self-inductance and resistance profile of first-stage winding; (solid line) conventional generator; (dashed line) generator with added resistance and time-varying L_P.

The procedure of the inductance calculation for this case, is similar to previously described in Section III. The only difference is that L_p must be time varying and burns out after generator operation. As we can see, self-inductance tends to zero at the end of generator operation while it reaches a non-zero value for conventional generator.

Since the first stage current passes a return conductor and does not get to load, its continuation causes more energy loss and decreases generator efficiency; therefore, this current should be interrupted after starting second stage operation. Sudden interruption of current may cause electrical break down in generator insulations [13]. It may be better to gradually decrease current of L_p using an incremental resistance in-series with that. In this paper a resistance increasing linearly from zero to 50 $m\Omega$ is added in-series with L_p. It is described how we can increase the resistance practically at the end of this section. Figure 6 shows the resistance profile of the first stage winding in the case of added resistance in comparison with conventional Cascaded-HFCG.

The equivalent electrical circuit of Cascaded-HFCG changes as Fig. 13 considering the proposed approach.
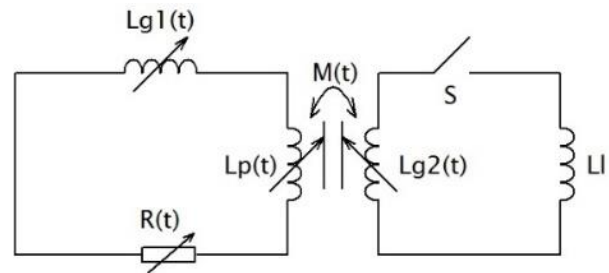

Fig. 7. Electrical circuit of cascaded-HFCG considering added resistance and dynamic L_p.

In order to validate the theoretical analysis performed in the previous section, a computer code is programmed based on the model demonstrated in Section II and electrical equivalent circuit of Fig. 7. A brief description of the modeled Cascaded-HFCG is needed here. The first stage winding is a single-pitch winding composed of 42 turns and has 300 mm length. Primary winding of dynamic transformer has 4 turns and 120 mm length. The inner diameter of first stage winding is 115 mm and the aluminum armature placed inside winding has an outer diameter of 50 mm. Armature wall thickness is 3.8 mm. The second stage winding has 30 turns and 120 mm length, which is located under first stage winding and ends at the same location as the ending of primary winding of dynamic transformer. The initial current of first stage winding is supplied by a 6 μF energy storage capacitor charged to about 20 KV. The load inductance is 25 nH. Detonation velocity is 6400 m/s.

Figure 8 shows the simulation results obtained from computer code for modeled Cascaded-HFCG. As we can see, current of first stage reaches a maximum value about 400 KA with rise time of current close to 65 μs, whereas maximum value of load current is 200 KA with rise time of current smaller than 15 μs for conventional generator. It is obvious that after starting second stage operation (about 50 μs) the current of first stage rises sharply and reaches an extremely high value. The reason for this excessive current is the high mutual inductance between the two windings and the energy returned to L_p, as previously discussed in detail.
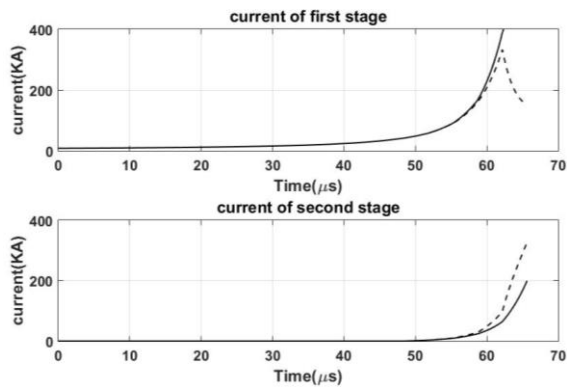
Fig. 8. Simulation results of conventional generator (solid line) and generator with time-varying L_P and incremental resistance (dashed line).

The simulation of the generator using the proposed method is done using self-inductance profile and resistance profile of first-stage winding, as demonstrated in Fig. 8. It can be seen that, after adding the resistance to the circuit, current of first stage follows a decreasing trend and causes an increase in load current. The maximum load current is 300 KA-i.e. 100 KA greater

than previous case. Current of first stage is limited to 300 KA due to the added resistance in-series with first stage winding. On the other hand, because of destructive behavior of L_p in this case and minimization of returned energy, the generator efficiency becomes greater. It is obvious that there is a considerable improvement in the di/dt and the rise time of the load current.

As we know, internal voltage in FCGs could reach about hundred kilovolts depending on some factors such as generator size, law of inductance change, and initial energy of system [17]. Actually, high internal voltages develop in HFCGs because of three reasons: high initial inductance of first stage winding, very small rise-time of current, and high value of inductance variation over time (dL/dt). For the proposed approach in this paper, dL/dt becomes greater than conventional Cascaded-HFCG because of the dynamic behavior of L_P, due to which the internal voltage becomes greater. Figure 9 shows internal voltage of the analyzed generator for two cases. The maximum value of internal voltage is 55 KV, which is much smaller than the critical value (critical value of internal voltage is 150 KV for HFCG [2]).
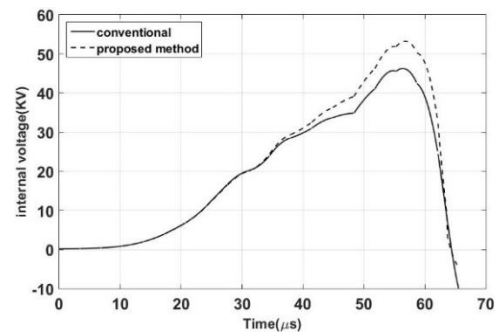
Fig. 9. Internal voltage for conventional generator (continued line) and proposed method (dashed line).

As for feasibility of the above behavior of incremental resistance and time varying L_P, it's better to describe the operation of a simple Exploded Opening Switch (EOS) first. The scheme of the device where current carrying foil is broken at its casting onto a ribbed dielectric barrier using high explosive (called EOS in literature) is shown in Fig. 10.
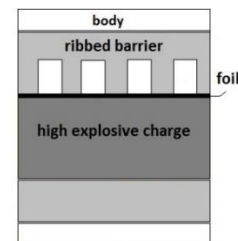
Fig. 10. Cross-section of exploded opening switch.

In the above described EOS, when the current carrying path is cut off by a ribbed barrier under the pressure of explosion, the current drops to zero sharply and a voltage surge is produced in the windings [12]. It may be better to find a way to increase the resistance slowly and simultaneous with armature expansion to prevent voltage surge formation in generator. In the following an approach is proposed to how we can increase the resistance in-series with first stage winding of Cascaded-HFCG gradually.
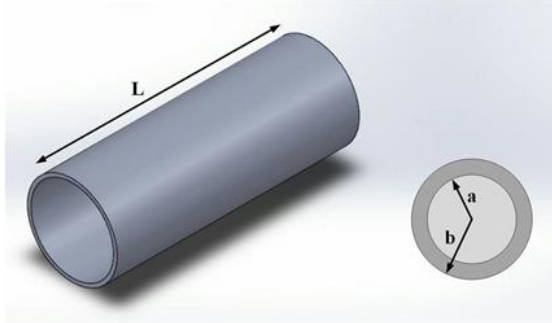

Fig. 11. Hollow cylinder conductor.

As we know, if a potential difference is applied to the ends of a hollow cylinder, electrical current can flow through its side surface azimuthally (Fig. 11). In this case, the cross-sectional area is $A = \pi(b^2 - a^2)$, thus the resistance is calculated from (19):

$$R = \rho \frac{L}{A} = \frac{\rho L}{\pi \left(b^2 - a^2 \right)},\tag{19}$$

From (19), the resistance of the cylinder is proportional to the length of conductor (L). If the cylinder is cut from one end helically, the length of the current carrying path increases, which causes an increase in resistance (Fig. 12).

Fig. 12. Cylindrical conductor which is cut helically.

In order to practical implement of the above-mentioned idea, we can consider a structure like that shown in Fig. 13.
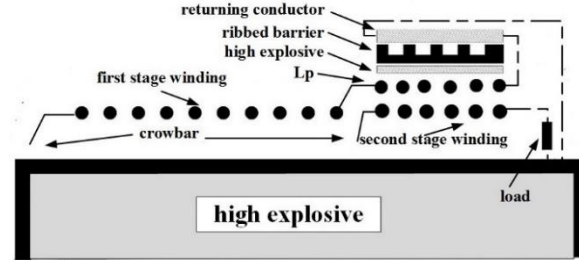

Fig. 13. Cascaded-HFCG with incremental resistance and time-varying L_P.

As we can see, a very thin hollow cylinder which is located over the L_P winding and coaxial with it, is considered as the returning conductor. The returning conductor is connected to L_p winding from one hand and to armature from the other hand. A ribbed barrier with helical grooves is located under the returning conductor which is faced to cylinder. The ribbed barrier is placed on explosive substrate. Detonation in substrate is initiated by an impact from expanding armature. The detonation propagates along cylinder and barrier, so pushed the grooves on the cylinder. Under the pressure of the grooves, the cylinder is cut in the form of helical and cause to an increase in the length of current path. Figure 14 shows a cross sectional representation of the ribbed barrier with helical grooves which can be used for our purpose. The ribbed barrier can be located over the cylindrical conductor too. In this case, the explosive charge should be located inside the cylindrical conductor. The mechanism of this device is similar to the EOS presented in Fig. 10.
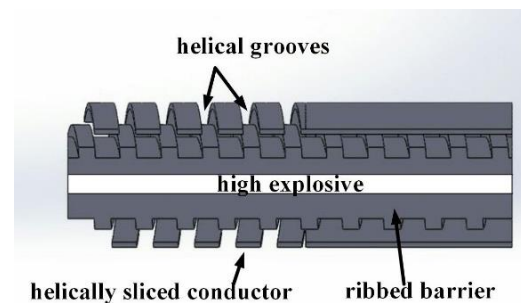

Fig. 14. Cross section of the ribbed barrier with helical grooves.

VI. CONCLUSION

Based on an analytical analysis, a new approach is proposed to improve the performance of Cascaded-HFCG. According to the proposed approach, each turn of the primary winding of the dynamic transformer should be wiped out simultaneously with armature expansion. This causes the primary winding to decouple from the secondary winding, which minimizes energy returning to the primary winding. On the other hand, a

gradually incremental resistance should be added in-series with the primary winding of the dynamic transformer. Added resistance restricts current increasing in primary winding, which causes lower energy loss, greater load current, and shorter pulse width of current. A quick numerical model is used to validate the performance of the proposed approach. Self-inductance and mutual inductance of the winding are calculated using FEM and compared to the results obtained by the 2-D filamentary method. FEM is an accurate and very fast method to calculate time-varying inductances in HFCGs.

REFERENCES

[1] L. L. Altgilbers, M. D. Brown, I. Grishnaev, B. M. Novac, I. R. Smith, I. Tkach, and Y. Tkach, *Magnetocumulative Generators*, Springer-Verlag, New York, 1999.

[2] A. A. Neuber (Editor), *Explosivley Driven Pulsed Power, Helical Magnetic Flux Compression Generators*, Springer-Verlag, Berlin, 2005.

[3] R. S. Caird and C. M. Fowler, "Conceptual design for a short-pulse explosive-driven generator," *Proc. 4th Megagauss Magnetic Field Generation and Pulsed Power Applications*, pp. 425, 1986.

[4] B. L. Freeman, L. L. Altgilbers, A. D. Luginbill, and J. C. Rock, "Development of small, tapered stator helical magnetic flux compression generators," *Electromagnetic Phenomena*, vol. 3, no. 3 (11), 2003.

[5] V. K. Chernyshev, G. S. Volkov, V. A. Ivanov, and V. V. Vakharushev, "Study of basic regularities of formation of multi-MA-current pulses with short risetime by EMG circuit interruption," in *Megagauss Physics and Technology*, pp. 663-675, Boston, 1980.

[6] P. V. Duday, A. A. Zimenkov, V. A. Ivanov, A. I. Kraev, S. V. Pak, A. N. Skobelev, and A. Y. Fevralev, "Method of generating a mega-ampere current pulse to accelerate a liner by a magnetic field," *J. Appl. Mech. Tech. Phys.*, vol. 56, no. 1, pp. 103-107, 2015.

[7] S. D. Gilev and V. S. Prokopiev, "Generation of electromagnetic energy in a magnetic cumulation generator with the use of inductively coupled circuits with a variable coupling coefficient," *J. Appl. Mech. Tech. Phys.*, vol. 58, no. 4, pp. 571-579, 2017.

[8] D. Q. Chen, "Research on Dynamic-Cascaded Helical Explosively-Driven Magnetic Flux Compression Generators," *Ph.D. Dissertation*, Changsha, P. R. China, 2015.

[9] A. Young, A. Neuber, and M. Kristiansen, "Design consideration for flux-trapping helical flux compression generator energized by capacitive discharge," *Pulsed Power Conference (PPC)*, pp. 527-531, Chicago, 2011.

[10] A. Young, A. Neuber, and M. Kristiansen, "Modeling and simulation of simple flux-trapping FCGs utilizing PSpice software," *IEEE Trans. Plasma Sci.*, vol. 38, no. 8, Aug. 2010.

[11] Y. Wang, J. Zhang, D. Chen, S. Cao, and D. Li, "Fast modeling of flux trapping cascaded explosively driven magnetic flux compression generators," *Rev. Sci. Instrum.*, 84, 014703, 2013.

[12] A. V. Shurupov, V. E. Fortov, A. V. Koslov, A. A. Leont'ev, N. P. Shurupova, V. E. Zavalova, S. V. Dudin, V. B. Mintsev, and A. E. Ushnurtsev, "Cascade explosive magnetic generator of rapidly increasing current pulses," in *14th International Conference on Megagauss Magnetic Field Generation and Related Topics*, pp. 1-5, 2012.

[13] A. A. Bazanov, "Helical magnetocumulative generators with magnetic flux amplification: comparative advantages of amplification schemes and the operational efficiency of generators with dynamic transformation," *Tech. Phys.*, vol. 56, no. 9, pp. 1339-1344, 2011.

[14] B. M. Novac and I. R. Smith, "A zero-dimensional computer code for helical flux-compression generators," *Electromagnetic Phenomena*, vol. 3, no. 4, 2003.

[15] B. M. Novac, I. R. Smith, M. C. Enache, and H. R. Stewardson, "2D modeling of inductively coupled helical flux-compression generators - FLUXAR systems," *Laser Part. Beams*, vol. 15, no. 3, pp. 397-412, 1997.

[16] M. H. Khanzade, Y. Alinejad-Beromib, and A. Shoulaie, "Calculation of time-varying equivalent inductance and resistance of helical flux compression generators using the 2D filamentary method and dynamic matrix concept in the frequency domain," *Chin. Phys. B*, vol. 19, no. 1, 2010.

[17] V. A. Demidov, "Problems of creation of high-efficient magnetocumulative generators electric strength of helical magnetocumulative generators," *IEEE Trans. Plasma Sci.*, vol. 38, no. 8, pp. 1773-1779, 2010.